TECHNICAL MEMORANDUM

249

On error growth in wave models

P. Janssen

Research Department

March 1998

European Centre for Medium-Range Weather Forecasts
Europäisches Zentrum für mittelfristige Wettervorhersage
Centre européen pour les prévisions météorologiques à moyen

On Error Growth in Wave Models

Peter Janssen

European Centre for Medium-Range Weather Forecasts

1. INTRODUCTION

In this note I would like to apply a simple duration-limited growth law for wind sea wave height to the problem of error growth in wave models. It will be shown that to a large extent this model is able to explain modelled wave height errors assuming that one knows the mean wind speed and the standard deviation of error in wind speed.

2. GROWTH LAW FOR WIND-DRIVEN SEA

A common view in the wave model community is that to a large extent wave height forecast errors are caused by wind speed forecast errors. This view is supported by *Cardone et al.* (1995) and by *Janssen et al.* (1997). In this note I present further support for this view by an analysis of wave and wind forecast scores from the ECMWF archives over the period August 1994 until November 1997.

We start from the basic premise that to a large extent wave height errors are caused by wind speed errors, and ask if this premise can provide an explanation of wave height error growth once wind speed errors are known. Since the 1940s and 1950s people have collected experimental evidence for a duration (and fetch) limited growth law for wind sea. Such a growth law relates a dimensionless wave height to a dimensionless wind speed. Based on duration limited WAM model data *Hersbach and Janssen* (1998) found the following growth law

$$H_S = \frac{\beta u_*^2/g}{(1 + T_{0*}/T_*)^{3/4}}, \qquad T_{0*} = 4.10^5, \tag{1}$$

where β is a constant (we use $\beta \approx 110$), u_* is the friction velocity, g is acceleration of gravity, and T_* is the dimensionless duration gT/u_* where T is the period over which the storm has blown. For infinite duration Eq. (1) becomes:

$$H_S = \beta u_*^2/g \tag{2}$$

in which case H_S is proportional to the square of the friction velocity. I make the basic assumption that all relevant quantities scale with the friction velocity and not with the wind speed at 10m height.

Friction velocity scaling has important consequences for our results on error growth. It was common in the past to base the wave evolution laws on wind speed scaling rather than friction velocity scaling, following the work of *Pierson and Moskovitz* (1964) on the equilibrium spectrum of wind waves. Their results were based on the analysis of *Kitaigorodskii* (1962) who argued that the most appropriate scaling parameter would be the friction velocity. Since this parameter was so difficult to measure in those days *Pierson and Moskovitz* compromised by choosing the wind speed at the then average height of the bridge of a ship (~ 19.5m). Later the wind speed at the standard height of 10m was chosen. *Janssen, Komen and de Voogt* (1987) pointed out that there are important differences between wind speed scaling and friction velocity scaling. The starting point of their investigation was a well-known discrepancy that existed in the 1970s between saturation levels for wind sea as observed during JONSWAP and as observed by KNMI. In case of wind speed scaling one would have

$$H_S = \alpha U_{10}^2/g \tag{3}$$

and one would expect α to be a constant. However, the JONSWAP observations, which were obtained during the Summer season, suggested that $\alpha \approx 0.14$ while the KNMI observations, obtained during the Winter season, gave a value of 0.22. *Janssen et al.* (1987) suggested that the discrepancy could be removed by adopting friction velocity scaling. In order to see this I introduce the drag coefficient C_D, where according to the field observations of e.g. *Smith* (1980) and many other works, the drag coefficient increases with wind speed,

$$C_D = a + bU_{10} \tag{4}$$

Note that in general C_D also depends on the sea state but since our interest is in the explanation of monthly mean errors we shall use a drag coefficient which is averaged over all possible sea states. An example is given in Fig. 1 and is obtained by averaging WAM model drag coefficients for each fixed wind speed (using a bin width of 0.1m/s). Remarkably, the average C_D follows very closely a linear law of the type given in Eq. (4). Eliminating from Eq. (2) the friction velocity through $u_*^2 = C_D U_{10}^2$ we obtain the dependence of wave height on wind speed if friction velocity scaling gives the universal asymptotic limit for wave height. We thus have

$$H_S = \beta C_D U_{10}^2/g \tag{5}$$

Hence in this case the proportionality parameter βC_D depends on wind speed, while in the case of wind speed scaling the parameter a is assumed to be constant. Since over the wind speed range of 5 to 20 m/s C_D varies by a factor of two it is clear that the choice of the velocity scale has important consequences for wave prediction. Using friction velocity scaling, Janssen et al. (1987) could explain the differences in the JONSWAP and KNMI data sets. The mean wind speed for the KNMI data was 15.1 m/s while for the JONSWAP data the mean wind speed was 9.1m/s. For the JONSWAP data set which was acquired during the summertime *Wu's* (1982) relation for the drag coefficient seems appropriate, i.e. in (4) we have

$$a = 0.8 10^{-3}, \qquad b = 0.065 10^{-3}, \tag{6}$$

and therefore for JONSWAP the mean drag coefficient would be 1.39 10^{-3}. The KNMI data set was obtained during the wintertime and in that period of the year wind seas are rougher because young wind seas occur more frequently. From the HEXOS data set (which was obtained in late Autumn) one may infer a mean Charnock parameter of 0.031. When fitting the linear relation (4) to the winter cases this gives

$$a = 0.8 10^{-3}, \qquad b = 0.09 10^{-3}, \tag{7}$$

and therefore for the KNMI data set the mean drag coefficient is 2.15 10^{-3}. The difference in mean drag coefficient between JONSWAP and the KNMI data set is sufficient to explain the differences in saturation level for wave height as the ratio of the two mean drag coefficients (JONSWAP over KNMI) is about 0.65.

Apart from considerations of a theoretical nature (cf. *Komen et al.* (1997)) the explanation of the differences between the JONSWAP and KNMI data set supports the use of friction velocity scaling. Additional support for friction velocity scaling comes from the observations of *Ewing and Laing (*1976) who collected data on fully developed wind seas from a buoy in the North Atlantic. *Blake* (1991) found the following dependence of saturation wave height on wind speed

$$H_S = 10^{-3}(8.7 + 0.73U_{10})U_{10}^2 \tag{8}$$

which closely resembles the scaling law for wave height obtained with friction velocity scaling. In order to see this we use *Wu*'s coefficients (Eq. (6)) combined with (5) to obtain

$$H_S = 10^{-3}(10.4 + 0.84U_{10})U_{10}^2 \tag{9}$$

In agreement with our findings regarding the JONSWAP and KNMI data set we see once more that the *Ewing and Laing* data set also shows a dimensionless saturation level for wave height, i.e. gH_S/U_{10}^2 which depends on wind speed. In particular, for winds in the range of 7m/s (which is the climatological mean) the dimensionless saturation level becomes according to (8) about 0.14 (in agreement with JONSWAP!) which is 60% lower than used in present day second generation wave models.

3. A STATISTICAL MODEL FOR WAVE HEIGHT ERROR GROWTH

Having motivated the choice of friction velocity scaling I now return to the model for forecast error growth. We write Eq. (1) as:

$$H = u_*^2 f \tag{10}$$

where $f = \beta/g(1 + T_{0*}/T_*)^{3/4}$

We would like to relate wind speed forecast errors to wave height forecast errors and therefore, using (10), we expand the wave height according to

$$\delta H = a\delta U_{10} + \frac{b}{2}\delta U_{10}^2 + \frac{c}{6}\delta U_{10}^3 + \ldots \tag{11}$$

where we disregard the higher order terms in the expansion because in the average rms error of wave height we only will include moments up to fourth order. The coefficients a, b and c which depend on the mean wind speed and the duration, may be found in the appendix.

We intend to apply our error growth model to the ECMWF monthly forecast verification statistics where the forecast is verified against analysis, which are available from 1994. The verification scores refer to standard deviation of errors and therefore we shall subtract the biases, i.e. we introduce

$$\delta H = \delta H - \langle\delta H\rangle, \qquad \delta u = \delta U_{10} - \langle\delta U_{10}\rangle \tag{12}$$

where a bracket denotes averaging. For example, from (11) we find

$$\langle\delta H\rangle = a\langle\delta U_{10}\rangle + \frac{b}{2}\langle\delta U_{10}^2\rangle + \frac{c}{6}\langle\delta U_{10}^3\rangle \tag{13}$$

And as a consequence we find for δh

$$\delta h = a\delta u + \frac{1}{2}b[2\delta u\langle\delta U_{10}\rangle + \delta u^2 - \langle\delta u^2\rangle] + \frac{1}{6}c[3\langle\delta U_{10}\rangle(\delta u^2 - \langle\delta u^2\rangle) + 3\langle\delta U_{10}\rangle^2\delta u + \delta u^3 - \langle\delta u^3\rangle] \tag{14}$$

As a result the standard deviation of wave height error follows from

$$\langle\delta h^2\rangle = \langle\delta u^2\rangle[a^2 + 2ab\langle\delta U_{10}\rangle + ac\langle\delta U_{10}\rangle^2 + b^2\langle\delta U_{10}\rangle^2] + \langle\delta u^2\rangle^2[\mathrm{ac} + \frac{1}{2}b^2] \tag{15}$$

We have retained contributions from the third and fourth moments because the deviation δu may be quite large. To evaluate these moments we assume that the probability distribution of the wind speed errors is approximately Gaussian and thus

$$\langle\delta u^3\rangle = 0; \qquad \langle\delta u^4\rangle = 3\langle\delta u^2\rangle^2$$

To show that the wind speed errors are approximately Gaussian we make the usual assumption that the wind component errors are Gaussian. The wind speed error is defined as the difference between forecast speed $r_f = \sqrt{u_f^2 + v_f^2}$ and analysed speed $r_a = \sqrt{v_a^2 + v_a^2}$, hence

$$\delta r = r_f - r_a = \sqrt{(\delta u + u_a)^2 + (\delta v + v_a)^2} - \sqrt{u_a^2 + v_a^2} \tag{16}$$

where δu and δv have a Gaussian distribution. Assuming that δu and δv are small compared to the analysed speed one may perform a Taylor expansion. At the same time introducing polar coordinates

$$\begin{aligned} \delta u &= \rho\cos\theta, & \delta v &= \rho\sin\theta, \\ u_a &= r_a\cos\phi, & v_a &= r_a\sin\phi, \end{aligned} \tag{17}$$

(Note that for Gaussian variables δu and δv the amplitude ρ is Rayleigh distributed while the phase θ is uniform) one finds to third order in $\varepsilon = \rho/r_a$

$$\delta r = r_a\left\{\varepsilon\cos\alpha + \varepsilon^2\left[\frac{1}{2} - \frac{1}{2}\cos^2\alpha\right] + \varepsilon^3\left[\frac{1}{2}\cos^3\alpha - \frac{1}{2}\cos\alpha\right] + O(\varepsilon^4)\right\} \tag{18}$$

where α = θ-ϕ. It follows now immediately that the wind speed error distribution is approximately Gaussian. This can be seen by retaining in (18) only the term linear in ε realising that ε is Rayleigh and α is uniform. However, there are also deviations from normality which may be important, thus we shall use the full expansion in (18) to evaluate the moments.

It is remarked that δr has a nonzero bias; averaging (18) one finds

$$<\delta r> = \frac{1}{4} r_a <\varepsilon^2>$$

Since in Eq. (17) we deal with the unbiased variable δu we correct for this by studying the moments of $\delta x = \delta r - <\delta r>$ instead, where

$$\delta x = r_a \left\{ \varepsilon \cos\alpha + \varepsilon^2 \left[\frac{1}{2} - \frac{1}{2}\cos^2\alpha \right] - \frac{1}{4}<\varepsilon^2> + \frac{\varepsilon^3}{2}[\cos^3\alpha - \cos\alpha] \right\} \tag{19}$$

The relevant moments now become

$$<\delta x> = 0$$

$$<\delta x^2> = r_a^2 \left\{ \frac{1}{2}<\varepsilon^2> - \frac{1}{16}<\varepsilon^2>^2 - \frac{1}{32}<\varepsilon^4> \right\} + O(\varepsilon^6)$$

$$<\delta x^3> = 0 + O(\varepsilon^6)$$

$$<\delta x^4> = \frac{3}{8} r_a^4 <\varepsilon^4> + O(\varepsilon^6)$$

The mean values $<\varepsilon^2>$ and $<\varepsilon^4>$ are determined using the Rayleigh distribution. In particular, one finds $<\varepsilon^4> = 2<\varepsilon^2>^2$ and this then finally enables us to express the higher moments in terms of the second moment. We thus have

$$\begin{aligned} <\delta x^2> &= r_a^2 \left\{ \frac{1}{2}<\varepsilon^2> - \frac{1}{8}<\varepsilon^2>^2 \right\} + O(\varepsilon^6) \\ <\delta x^4> &= 3<\delta x^2>^2 + O(\varepsilon^6) \end{aligned} \tag{20}$$

The last equation is the usual one that follows from the Gaussian approximation, and has been used in deriving the main result of this note, namely Eq. (15).

We now verify (15) by comparing actual wave height errors with errors obtained from (15). At ECMWF monthly mean forecast scores against analysis for surface wind and wave height are produced on a regular basis. The forecast range is 10 days. Fig.2 shows a plot of the standard deviation of wave height error versus the standard deviation of wind speed error for the North Atlantic(o), North Pacific(Δ), Tropics($\Diamond$) and the Southern Hemisphere(∇). Fig. 2 shows a close relationship between the wind speed and wave height error. The relationship seen in Fig. 2 is much clearer than that found by comparing modelled wave height with buoy observations (*Janssen et al.*, 1984). An even better fit is obtained when using the error model (15). To that end, we substituted in Eq. (15) mean wind, mean error of wind and standard deviation of wind error and assumed C_D a function of U_{10} with coefficients

$$a = 0.6\ 10^{-3}$$

$$b = 0.09\ 10^{-3}$$

as obtained from the relation of WAM C_D versus wind speed displayed in Fig. 1. In addition, we assumed an average duration of the wind seas of 12 hours. The result for the North Atlantic and the North Pacific is given in Fig. 3 where we plot on the x-axis the verification scores for wave height s.d. error from the ECMWF archive over the last 3 years while on the y-axis the wave height error according to Eq. (15) is plotted. There is a remarkable agreement between the error model of Eq. 15 and the forecast verification scores (correlations are about 98% for a linear fit). Our error model is quite sensitive to the choice of the relation for the drag coefficient and to the choice of the average duration of wind sea. In particular, the choice of a duration of 12 hours may seem rather short. To investigate whether the choice was reasonable I retrieved for one synoptic time the wind sea wave heights, wind speeds and drag coefficients from ECMWF's daily archive, and determined the duration of wind sea using Eq. (1). Remarkably, for the North Atlantic the average duration was 12 hours while for the North Pacific it was 14 hours. As a result, mean drag coefficients for high wind speeds were lower in the North Pacific than in the North Atlantic. We conclude that the choice of a duration of 12 hours is not unreasonable.

The higher moments in (15) play an important role, in particular for the higher values of the wave height error. These higher moments are the main reason that the relation between our error model and the forecast scores is so linear (which contrasts with the relation between wave height error and wind speed error in Fig. 2). In addition, the higher moments reduce the scatter to a considerable extent, as illustrated in Fig. 4 for the North Atlantic area where we compare results of Eq. (15) with the simple linear model

$$<\delta h^2> = a^2 <\delta u^2>$$

which disregards the effects of the third and fourth moments.

4. CONCLUSION

We have introduced a simple model for the wave height error which is based on a duration limited growth law for wind driven wind sea. The model has been applied to the forecast verification scores of the ECMWF wave forecasting system and it is seen that the error model shows remarkable skill in explaining the results for the standard deviation of wave height error. These verification scores have been obtained by comparing the wave forecast with the analysis. In general one would expect the wave height error to contain two components namely an internal wave model error (errors in the source terms, swell errors caused by propagation) and an external error related to wind field inaccuracies. Since both analysis and forecast have similar internal wave model errors, the forecast verification scores mainly show external wind speed errors. This is supported by the present analysis. Furthermore, *Janssen et al.* (1997) have shown that based on verifications of wave forecasts against buoy data, the external wind speed errors dominate the wave height error from day 2 onwards while even in the analysis and short range forecast the internal wave model errors play a minor role.

Assuming that we have a valid model for error growth an important consequence may be pointed out regarding the skill of a wave forecast model. This is most easily seen for steady state conditions when the wind sea wave height is given by (cf. Eq. (5))

$$H_S = \frac{\beta}{g} C_D U_{10}^2$$

Wave height errors are small when the drag coefficient C_D is small. On the other hand, a reasonable value for CD is required in order to obtain realistic results for extreme conditions. Now, wave models such as the WAM model (which is based on friction velocity scaling) have a reasonably good forecast skill because the bulk of the data is obtained at relatively low wind speed which corresponds to a low drag coefficient. As a result the wave height error is small. The skill of wave forecast models that use wind speed scaling, hence constant C_D, is expected to be worse. In order to treat the extreme events in a satisfactory way a high drag coefficient is required, but as a consequence the result is a relatively high wave height error as well.

REFERENCES

Blake, R.A., 1991, The dependence of wind stress on wave height and wind speed, *JGR* 96, 20, 531-20, 543.

Cardone, V.J., H.C. Graber, R.E. Jensen, S. Hasselmann and M.J. Caruso, 1995, In search of the true surface wind field in SWADE IOP-1: Ocean wave modelling perspective. *The Global Atmosphere and Ocean System*, **3**, 107-150.

Charnock, H, 1955, Wind stress on a water surface. *Q.J.Royal Meteorol.Soc.*, **81**, 639-640.

Ewing, J. and Laing, 1976, *J. of Phys. Oceanogr.*, **19**, 1696-1706.

Hersbach, H.A. and P.A.E.M. Janssen, 1998. Improvement of Short Fetch behaviour in the WAM model, submitted to *Journal of Atmosph. And Ocean. Tech.*, 1998

HEXOS: Smith, S.D., R.J. Anderson, W.A. Oost, C. Kraan, N.Maat, J. De Cosmo, K.B. Katsaros, K.L. Davidson, K. Bumke, L. Hasse and H.M. Chadwick, 1992. Sea surface wind stress and drag coefficients: the HEXOS results. *Boundary Layer Meterol.*, **60**, 109-142

Janssen, P.A.E.M., G.J.Komen and W.J.P. de Voogt, 1987. Friction velocity scaling in wind-wave generation. *Boundary Layer Meteorol.*, **38**, 29-35

Kitaigorodskii, S.A., 1962, Application of the theory of Similarity for the analysis of wind-generated water waves as a stochastic process. *Bull Acad. Sci USSR Geophys.*, Ser. no. **1**, 730

Komen, G.J., L, Cavaleri, M. Donelan, K. Hasselmann, S. Hasselmann and P.A.E.M. Janssen, 1994, *Dynamics and Modelling of Ocean Waves*, CUP, Cambridge.

Pierson, W.J., Jr. and L. Moskovitz, 1964. A proposed spectral form for fully developed wind seas based on the similarity theory of S.A. Kitaigorodskii, *J. Geophys. Res.*, **69**, 5181.

Smith, S.D., 1980, Wind Stress and Heat flux over the ocean in Gale Force Winds, *J.Phys. Oceanogr.*, **10**, 709-726

Wu, J, 1982, Wind - Stress Coefficients over Sea Surface from Breeze to Hurricane, *J.Geophys. Res.*, **87**, 9704-9706

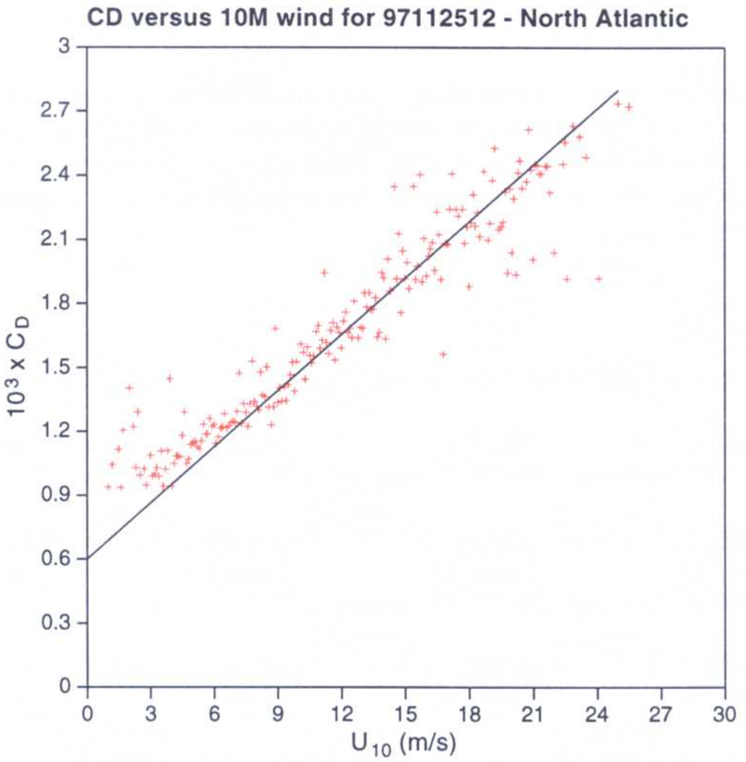

Figure 1 Average drag coefficient from the WAM model as function of wind speed. Area is North Atlantic.

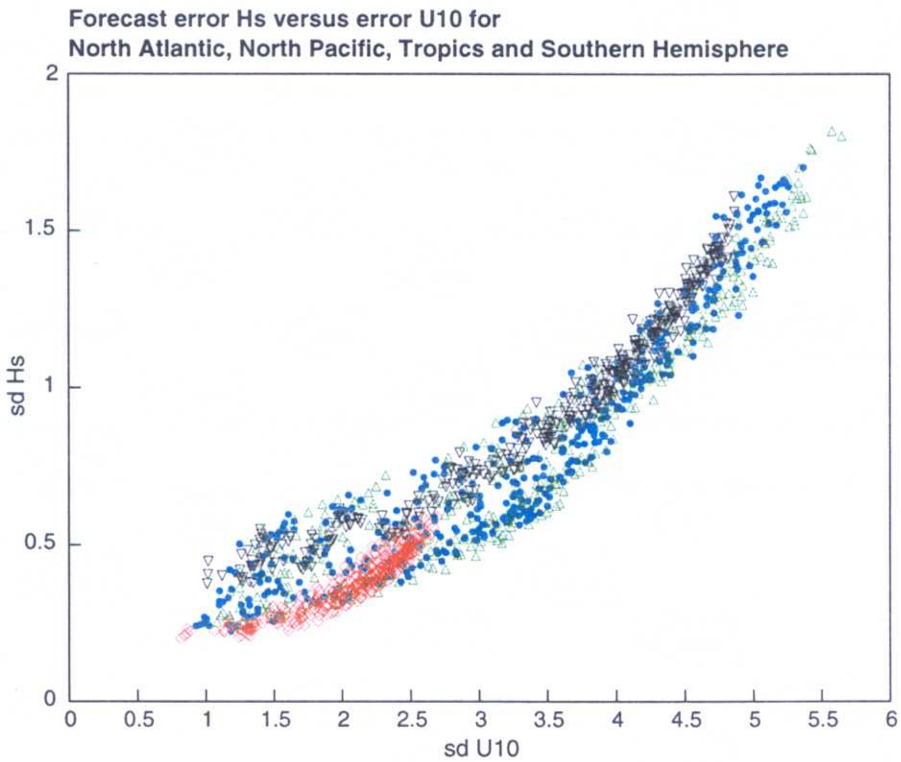

Figure 2 Forecast error in wave height as function of forecast error in wind speed for 4 different areas. (North Atlantic (O), North Pacific (△), Tropics (◇) and Southern Hemisphere (△)). The data cover the forecast range between 12 hours and 10 days.

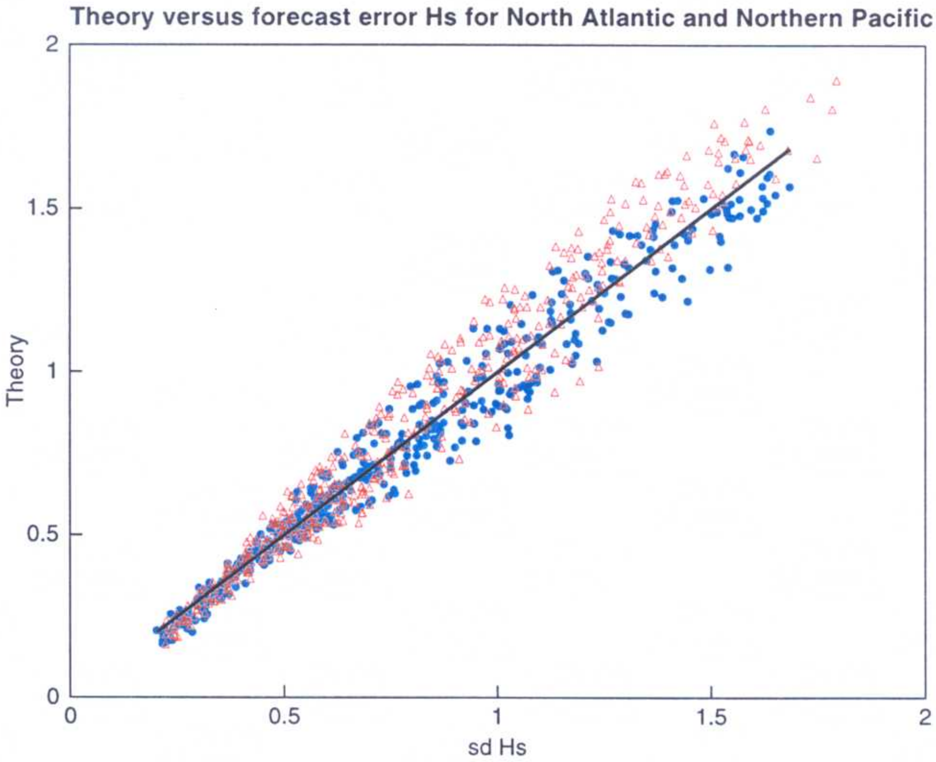

Figure 3 Theoretical estimate of wave height forecast error versus actual wave height error for North Atlantic (O) and North Pacific (Δ).

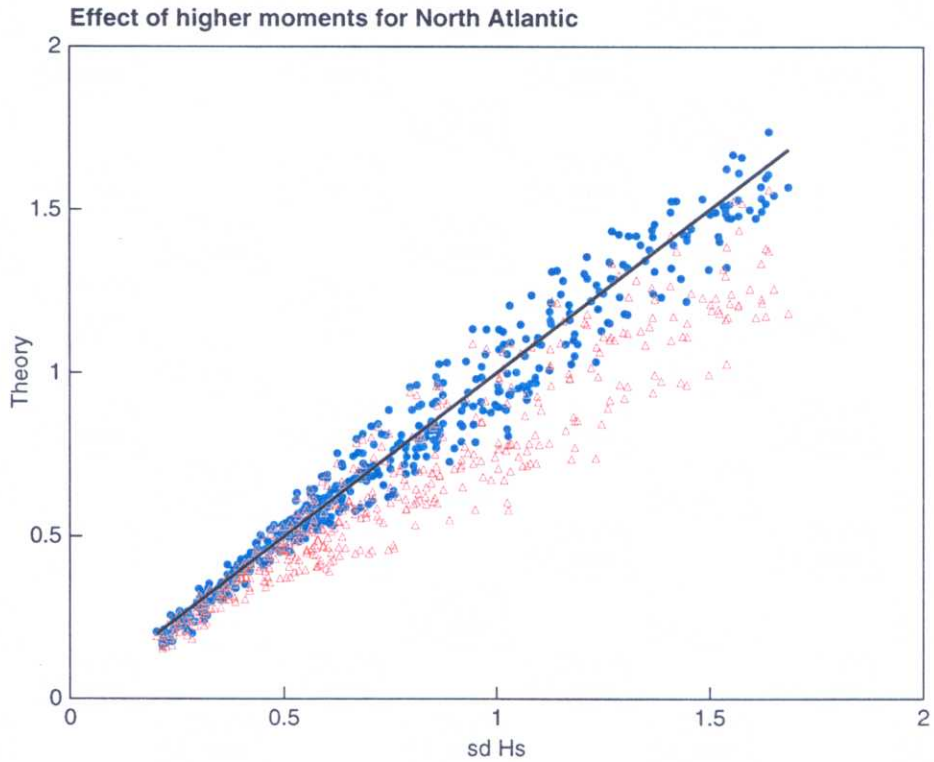

Figure 4 Effect of neglecting the third and fourth moment, shown for the North Atlantic (O) including higher moments, (Δ) neglecting higher moments.

APPENDIX

Using (10) we find for a, b and c the following chain of relations.

$$
\begin{aligned}
a &= \frac{\partial H}{\partial U_{10}} = \frac{\partial H}{\partial u_*}\frac{\partial u_*}{\partial U_{10}} \\
b &= \frac{\partial^2 H}{\partial U_{10}^2} = \frac{\partial H}{\partial u_*}\frac{\partial^2 u_*}{\partial U_{10}^2} + \frac{\partial^2 H}{\partial u_*^2}\left(\frac{\partial u_*}{\partial U_{10}}\right)^2 \\
c &= \frac{\partial^3 H}{\partial U_{10}^3} = \frac{\partial H}{\partial u_*}\frac{\partial^3 u_*}{\partial U_{10}^3} + 3\frac{\partial^2 H}{\partial u_*^2}\frac{\partial u_*}{\partial U_{10}}\frac{\partial^2 u_*}{\partial U_{10}^2} + \frac{\partial^3 H}{\partial u_*^3}\left(\frac{\partial u_*}{\partial U_{10}}\right)^3
\end{aligned}
\tag{A.1}
$$

Here, assuming that C_D depends linearly on U_{10}, we have:

$$
\begin{aligned}
\frac{\partial u_*}{\partial U_{10}} &= C_D^{1/2}(1+A) \\
\frac{\partial^2 u_*}{\partial U_{10}^2} &= C_D^{-1/2}\frac{\partial C_D}{\partial U_{10}}\left(1-\frac{1}{2}A\right) \\
\frac{\partial^3 u_*}{\partial U_{10}^3} &= -\frac{3}{4}C_D^{-3/2}\left(\frac{\partial C_D}{\partial U_{10}}\right)^2(1-A)
\end{aligned}
$$

with $A = \frac{1}{2}\frac{U_{10}}{C_D}\frac{\partial C_D}{\partial U_{10}}$ while

$$
\begin{aligned}
\frac{\partial H}{\partial u_*} &= 2u_*f + u_*f' \\
\frac{\partial^2 H}{\partial u_*^2} &= 2f + 4u_*f' + u_*^2 f'' \\
\frac{\partial^3 H}{\partial u_*^3} &= 6f' + 6u_*f'' + u_*^2 f'''
\end{aligned}
$$

where (with m = 3/4)

$$u_*f' = -m\frac{\beta}{g}\frac{T_0}{T_*}\left(1+\frac{T_0}{T_*}\right)^{-m-1}$$

$$u_*^2 f'' = m(m+1)\frac{\beta}{g}\left(\frac{T_0}{T_*}\right)^2\left(1+\frac{T_0}{T_*}\right)^{-m-2}$$

$$u_*^3 f''' = -m(m+1)(m+2)\frac{\beta}{g}\left(\frac{T_0}{T_*}\right)^3\left(1+\frac{T_0}{T_*}\right)^{-m-3}$$